Species limits, interspecific hybridization and phylogeny in the cryptic land snail complex Pyramidula : the power of RADseq data

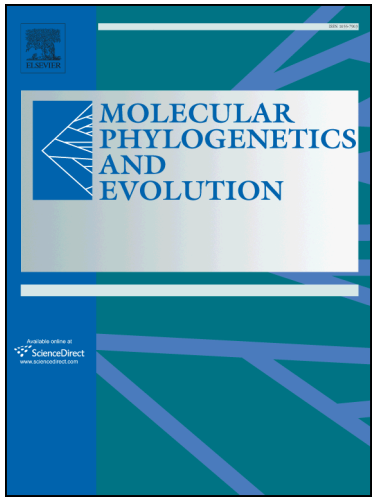

Species limits, interspecific hybridization and phylogeny in the cryptic land snail complex *Pyramidula*: The power of RADseq data

Oihana Razkin, Gontran Sonet, Karin Breugelmans, María José Madeira, Benjamín Juan Gómez-Moliner, Thierry Backeljau

PII: S1055-7903(16)30083-5
DOI: http://dx.doi.org/10.1016/j.ympev.2016.05.002
Reference: YMPEV 5511

To appear in: *Molecular Phylogenetics and Evolution*

Received Date: 5 April 2016
Revised Date: 24 April 2016
Accepted Date: 1 May 2016

Please cite this article as: Razkin, O., Sonet, G., Breugelmans, K., Madeira, M.J., Gómez-Moliner, B.J., Backeljau, T., Species limits, interspecific hybridization and phylogeny in the cryptic land snail complex *Pyramidula*: The power of RADseq data, *Molecular Phylogenetics and Evolution* (2016), doi: http://dx.doi.org/10.1016/j.ympev.2016.05.002

Title:

Species limits, interspecific hybridization and phylogeny in the cryptic land snail complex *Pyramidula*: the power of RADseq data

Author names and affiliations:

Oihana Razkin[a], Gontran Sonet[b], Karin Breugelmans[b], María José Madeira[a], Benjamín Juan Gómez-Moliner[a], Thierry Backeljau[b,c]

[a] Department of Zoology and Animal Cell Biology, Faculty of Pharmacy, University of the Basque Country (UPV/EHU), Paseo de la Universidad 7, 01006 Vitoria-Gasteiz, Alava, Spain; Biodiversity Research Group CIEA Lucio Lascaray, Avda. Miguel de Unamuno 3, 01006, Alava, Spain. E-mail: oihana.razkin@ehu.es, mariajose.madeira@ehu.es, benjamin.gomez@ehu.es.

[b] Royal Belgian Institute of Natural Sciences (OD Taxonomy and Phylogeny & JEMU), Vautierstraat 29, B-1000 Brussels, Belgium. E-mail: gontran.sonet@naturalsciences.be, karin.breugelmans@naturalsciences.be, thierry.backeljau@naturalsciences.be.

[c] Evolutionary Ecology Group, University of Antwerp, Groenenborgerlaan 171, B-2020 Antwerp, Belgium.

Corresponding autor:

Oihana Razkin. Department of Zoology and Animal Cell Biology, Faculty of Pharmacy, University of the Basque Country (UPV/EHU), Paseo de la Universidad 7, 01006 Vitoria-Gasteiz, Alava, Spain. E-mail: oihana.razkin@ehu.es Phone number: 00 34 945 013043.

Abstract:

Restriction site-associated DNA sequencing (RADseq) was used to jointly assess phylogenetic relationships, interspecific hybridization and species delimitation in the cryptic, non-model land snail complex *Pyramidula*. A robust phylogeny was inferred using a matrix of concatenated sequences of almost 1,500,000 bp long, containing > 97,000 polymorphic sites. Maximum likelihood analyses fully resolved the phylogenetic relationships among species and drastically improved phylogenetic trees obtained from mtDNA and nDNA gene trees (COI, 16S rRNA, 5.8S rRNA, ITS2 and 28S rRNA sequence data). The best species delimitation scenario was selected on the basis of 875 unlinked single nucleotide polymorphisms, showing that nine *Pyramidula* species should be distinguished in Europe. Applying D-statistics provided no or weak evidence of interspecific hybridization among *Pyramidula*, except for some evidence of gene flow between two species.

Keywords:

Restriction-site associated DNA sequencing; phylogeny; interspecific hybridization; species delimitation; *Pyramidula*

1. Introduction

The inference of phylogenetic relationships among closely related, recently diverged, non-model species is a challenging problem (Maddison and Knowles, 2006), because either there are no good phylogenetic markers available or those that are available contain insufficient phylogenetic signal. Moreover, different gene trees of closely related taxa may show conflicting topologies due to interspecific gene flow or incomplete lineage sorting (Maddison, 1997; Wendel and Doyle, 1998; Degnan and Rosenberg, 2009). The inference of species trees from multilocus data can help to distinguish these two processes (Kubatko, 2009; Yu et al., 2011). Unfortunately, obtaining multiple informative markers for non-model species is not a straightforward task (Schlötterer, 2004; Thomson et al., 2008).

Current high-throughput sequencing technologies allow gathering large scale genome-wide data at moderate to low costs. As such, they are increasingly applied to address phylogenetic problems (Emerson et al., 2010; Eaton and Ree, 2013; Wagner et al., 2013; Hipp et al., 2014; Takahashi et al., 2014). This is particularly true for Restriction-site associated DNA sequencing (RADseq; Baird et al., 2008; Davey and Blaxter, 2010), a technique that can be applied to non-model organisms for which there is no reference genome data available. Reduced genomic representation in RADseq is achieved by sampling only at specific sites in the genome defined by restriction enzymes, which in turn allows the identification of thousands of genetic markers across the genome in many individuals (Davey and Blaxter, 2010).

RADseq allows (1) creating phylogenetic datasets of unprecedented size (Eaton and Ree, 2013; Eaton, 2014; Escudero et al., 2014; Hipp et al., 2014; Takahashi et al., 2014), (2) genotyping thousands of SNP throughout the genome (Baird et al., 2008), (3) detecting hybridization and introgression among non-model organisms (Twyford and Ennos, 2011; Eaton and Ree, 2013), and (4) applying new methods for inferring species trees and species delimitation (Leaché et al., 2014). Therefore, RADseq may be a promising tool to assess species limits and phylogenetic relationships in closely related taxa for which traditional DNA sequence approaches have failed to provide well-supported solutions.

The land snail genus *Pyramidula* Fitzinger, 1833 is a challenging case for the application of RADseq. It is a non-model species complex distributed over almost all of Europe, the Mediterranean area, Central Asia and Japan (Gómez-Moliner, 1988; Welter-

Schultes, 2012). It comprises small species (diameter < 3 mm) with widely umbilicated, trochoid shells (Gittenberger and Bank, 1996). *Pyramidula* spp. inhabit limestone rocks (Gittenberger and Bank, 1996; Kerney, 1999; Martínez-Ortí et al., 2007) from sea level to altitudes of 3800 m (Schileyko and Balashov, 2012). During most of the 20th century, the genus was considered to contain one single species, *Pyramidula rupestris* (Draparnaud, 1801), until Gittenberger and Bank (1996) suggested that in Europe at least six species should be distinguished on conchological basis. However, the diagnostic shell characters highly relied on size and shape features, i.e. phenotypic features that may be plastic and hence that may be affected by environmental factors (Goodfriend, 1986; Heller, 1987; Harley et al., 2009; Stankowski, 2011).

In order to resolve the taxonomy of the *Pyramidula* complex, Razkin et al. (2016) applied an integrative taxonomic and species delimitation approach to analyse 211 specimens of *Pyramidula* collected throughout Europe and adjacent Mediterranean areas. Phylogenetic relationships and species boundaries were inferred on the basis of a multilocus DNA sequence dataset and niche modeling. In this way, nine putative *Pyramidula* species were distinguished in the western Palaearctic region. Phylogenetic reconstructions yielded good support values for species level clades, but not for species relationships. Moreover, the phylogenies based on mitochondrial (mtDNA) COI and 16S and nuclear (nDNA) 5.8S-ITS2-28S markers showed several unsupported branches and incongruent topologies. This latter observation was tentatively interpreted as the result of incomplete lineage sorting. Hence, further work involving more molecular markers was needed to assess whether, and to what extent, processes like interspecific gene flow or incomplete lineage sorting have shaped the phylogenetic relationships among *Pyramidula* species.

The present study addresses the problematic issues in the study of Razkin et al. (2016) by applying RADseq technology in order to 1) reconstruct the phylogenetic relationships within *Pyramidula*, 2) re-assess the delimitation of nine species, and 3) test whether interspecific gene flow or incomplete lineage sorting are responsible for the discordant mtDNA and nDNA gene trees of *Pyramidula*.

2. Materials and methods

2.1. Taxon sampling

We selected 25 individuals of *Pyramidula* from the study of Razkin et al. (2016) representing the nine putative species: *P. pusilla* (n = 4), *P. rupestris* (n = 3), *P. jaenensis* (n = 4), *P. chorismenostoma* (n = 1), *P. cephalonica* (n = 4), *P. saxatilis* (n = 2), *P.* cf. *hierosolymitana* (n = 2), *Pyramidula* sp1 (n = 1) and *Pyramidula* sp2 (n = 2). Two remaining individuals were conchologically characterized as *P. cephalonica*, but their mtDNA sequences were more similar to *P. chorismenostoma* than to *P. cephalonica*, and thus suggested possible interspecific hybridization or incomplete lineage sorting. The selection of the individuals was based on their geographic spread (Figure 1). Locality information is provided in Table 1. Genomic DNA extracts were already available from Razkin et al. (2016).

2.2. RAD sequencing

Two RAD libraries were prepared following the protocol of Baird et al. (2008) and Etter et al. (2011). We used a Qubit fluorimeter 2.0 (Life Technologies) to check that each DNA extract contained a minimum of 250 ng of genomic DNA per 35 µl. Each individual sample was digested for 60 min at 37 ºC with restriction enzyme SbfI (New England Biolabs; NEB). P1 adapters (IDT) containing a sample specific molecular identifier were ligated to each digested DNA sample. These barcoded samples were pooled in two libraries and purified using DNA Clean & Concentrator™-5 (Zymo Research). Each library was sheared to an optimal size of 400 bp (samples of 50 µl in microTUBE AFA Fiber Screw-Cap for 60 s using a focused-ultrasonicator M220, Covaris) followed by a size selection on gel. Libraries were then blunted with Quick Blunting Kit (NEB), followed by an A-tailing step. Afterwards, P2 adapters (IDT) were ligated and PCR amplification was performed using P1 and P2 primers with Phusion High-Fidelity Master Mix (Thermo-scientific). We used a Qubit fluorimeter 2.0 (Life Technologies) to check that the amount of DNA in the final amplified library increased by 1.5x and a 2100 Bioanalyzer system with a High Sensitivity DNA kit (Agilent Technologies) to check that the final fragment size was in the expected range of 300-400 bp. Each library was run in a single paired-end Illumina MiSeq lane flow cell (v2 kit 2 x 250 bp) at The GenePool facility (University of Edinburgh). We used the reads 1 (250 bp).

2.3. RADseq data processing

For the data analysis, we followed the pipeline implemented in the software *pyRAD* v. 3.0 (Eaton and Ree, 2013; Eaton, 2014). *pyRAD* assembles RADseq data into groups of

similar sequences that will be considered orthologs and treated as different loci without using a reference sequence (pipeline "*de novo"*). Compared to *Stacks* (Catchen et al., 2011), which does not consider indels and was developed for population level analyses, *pyRAD* was developed to search for homologies across more divergent samples (even among different species) and uses a clustering method (see below) that allows for indel variation.

pyRAD separated the reads of the 25 individuals using the sample specific molecular identifier barcodes that were attached during the library preparation. Base calls with a phred quality score below 20 were converted to Ns (undetermined sites) and reads including more than a maximum number of Ns were discarded (several maxima were tested, see below). Each read (250 bp) was reduced to 236 bp after removing the sample specific molecular identifier (8 bp) and restriction sites (6 bp). Filtered reads were clustered and aligned using the two programs that are implemented in the *pyRAD* pipeline, *vsearch* (https://github.com/torognes/vsearch) and *muscle* (Edgar, 2004). Consensus sequences kept information on heterozygous sites as ambiguity codes and those containing more than the allowed number of heterozygous sites (see below) or more than two haplotypes were discarded so as to eliminate paralogs (or repetitive or high copy number DNA regions).

The key parameters of *pyRAD* that can cause an under- or overmerging of clusters, and therefore may lead to misidentification of orthologous sequences, are the "clustering threshold" and the "minimum depth of coverage". The clustering threshold is the minimum percent similarity required by *vsearch* to consider sequences as orthologs. High similarity thresholds lead to a too strict identification of clusters (loci), so that orthologous loci with more variable sequences may be considered as different loci. Conversely, too low similarity thresholds will group orthologous loci with highly variable sequences, but may also include paralogous and other non orthologous loci in the same cluster (locus). The minimum depth of coverage is the minimum number of identical reads required to take a sequence into account. Low values for this parameter may increase the risk to include erroneous sequences in the analysis, while high values increase the risk to exclude orthologous loci with low coverage.

Catchen et al. (2013) stated that the optimal values for the "clustering threshold" and the "minimum depth of coverage" depend on the degree of polymorphism, the amount of sequencing error and the depth of coverage. They suggested testing a range of values for

each parameter for each dataset. Therefore, we performed 9 tests in *pyRAD* using three clustering thresholds (85%, 90% and 95%) and three depths of coverage (3, 5 and 7). Three other parameters ("Maximum number of undetermined sites in filtered sequences"; "Maximum number of Ns in a consensus sequence" and "Maximum number of heterozygous sites in a consensus sequence") were adjusted to each clustering threshold following the recommendations of the *pyRAD* manual. In further analyses, we used the output of the test that retained as many orthologous loci as possible so as to reduce the chance to include sequences with errors. Following Viricel et al. (2014) we looked at the resulting matrix length and the number of SNPs obtained with the set of the previously defined *pyRAD* parameters (coverage and similarity threshold). When a plateau was observed (less variation in the matrix length and the number of resulting SNPs for a larger variation in the *pyRAD* parameters), we used the largest *pyRAD* parameter in the window of this plateau. In this way, we reduce (but not exclude) the chance to include sequences with errors and minimise the risk of including non-orthologous sequences. For the parameter "Minimum taxon coverage" that specifies the minimum number of samples with data for a given locus to be retained in the final dataset, a value of 18 samples was applied for the 9 tests. With the aim to know how the variation of this parameter could affect the phylogenetic analyses, we modified this value (12, 18, 23 and 25) for one selected test.

For the remaining parameters default values were employed.

2.4. Phylogenetic inference

2.4.1. RADseq phylogeny

For the phylogenetic analyses we used the output of *pyRAD* which contained all the loci concatenated into one supermatrix. Maximum likelihood (ML) analyses were performed using RAxML v. 8.1.11 (Stamatakis, 2014) implemented at the CIPRES Science Gateway (Miller et al., 2010) applying a rapid bootstrapping analysis with 100 bootstrap pseudoreplicates and a general-time-reversible nucleotide substitution model. The analyses were performed for the supermatrix of each of the 11 tests (9 test values for "clustering threshold" and "minimum depth of coverage" and 2 extra tests values for "minimum taxon coverage"). The alignments of the 11 tests are provided in online Supplementary data 1 (awaiting repository number).

2.4.2. Five-gene phylogeny

We also reconstructed a phylogeny for the same 25 taxa included in the RADseq analysis, but with the COI, 16S rRNA, 5.8S rRNA, ITS2 and 28S rRNA sequence data of Razkin et al. (2016). The results of these analyses were compared with those obtained with the RADseq data.

Sequences were aligned with the online version of Mafft v.7 (Katoh and Standley, 2013). We used the Q-INS-i algorithm for rRNA, which considers the secondary structure of RNA (Katoh and Toh, 2008), and the Auto algorithm for COI. Default values were used for the remaining parameters. Numbers of variable sites were inferred using DnaSP v. 5.10.1 (Librado and Rozas, 2009). ML trees were reconstructed using three datasets: COI+16S (mitochondrial), 5.8S+ITS2+28S (nuclear) and all five fragments concatenated. Each dataset was partitioned according to the genes, and COI was further partitioned according to the three codon positions. ML trees were inferred with RAxML v. 8.1.11 (Stamatakis, 2014) with bootstrapping over 100 replicates and with the GTR substitution model for each partition.

Outgroup samples were not available for the RADseq data and hence, all phylogenies were midpoint rooted.

2.5. Species delimitation

We used the Bayes Factor Delimitation* (BFD*) method (Leaché et al., 2014) to compare several species delimitation scenarios. We first used SNAPP, a package for inferring species trees from unlinked biallelic markers (Bryant et al., 2012), to set up five hypothetical scenarios. Then, we ran BEAST 2 (Bouckaert et al., 2014) to calculate the marginal likelihoods of each scenario under the priors selected in SNAPP. Finally, we used BFD* to make pairwise comparisons among the marginal likelihoods obtained for the different scenarios.

2.5.1. SNAPP- prior selection

The dataset obtained with the *pyRAD* analysis (clustering threshold of 0.9 with a minimum depth of coverage of 5 = c90m5) was selected with the criteria described in 2.3 and was used to carry out SNAPP analyses. We did not allow for missing data (minimum taxon coverage = 25) and we obtained a subset of 368 SNPs that came from different reads that we considered as unlinked. If multiple SNPs were found in a locus, *pyRAD* sampled SNP sites randomly. In order to increase the number of unlinked SNPs, we also performed SNAPP analyses on another dataset (clustering threshold of 0.9 with

a minimum depth of coverage of 3 = c90m3, using minimum taxon coverage = 25), yielding 875 SNPs. The alignment of this dataset converted to biallelic markers is provided in online Supplementary data 2 (awaiting repository number).

For the ancestral population sizes a variety of theta values were tested, all of them with gamma distribution priors: Gamma (2, 200), Gamma (2, 2000) and Gamma (2, 20000) (Leaché et al., 2014). Priors were set to default values or calculated according to the manual. Each analysis was run in BEAST 2 (Bouckaert et al., 2014) for 1 million generations with sampling every 1000 generations. The first 10% iterations were discarded as burnin and convergence was confirmed by examining log files (ESS > 200).

Different prior distribution on theta yielded identical posterior probabilities (PP) in the species tree. The Gamma value (2, 2000) was retained for subsequent analysis. We found no topological and branch length differences between the analyses of c90m5 and c90m3. Therefore, we only reported the results of the largest dataset (c90m3) which was used in subsequent analyses for BFD*.

2.5.2. BFD - comparison between scenarios*

Marginal likelihoods of each scenario were estimated in BEAST 2 by conducting a path sampling method with 48 steps, each one consisting of 400,000 generations with a burnin value of 10%. Bayes Factors were calculated as twice the difference of the log marginal likelihoods of the two models used in the comparison (base scenario and alternative scenario). A positive Bayes Factor supports the base scenario, whereas negative values support the alternative model.

Our base scenario was the recognition of the nine species proposed by Razkin et al. (2016): *P. pusilla*, *P. rupestris*, *P. jaenensis*, *P. chorismenostoma*, *P. cephalonica*, *P. saxatilis*, *P.* cf. *hieroslymitana*, *Pyramidula* sp1 and *Pyramidula* sp2 (Figure 2a). Since it was not computationally feasible to test all possible scenarios we tested four alternative scenarios. In two of them we clustered closely related species based on the results of the phylogenetic inference: Clustering 1 (Figure 2b), in which *P. rupestris* + *P. saxatilis* were clustered as a single species and Clustering 2 (Figure 2c), in which *P. jaenensis* + *P. chorismenostoma* + *P. cephalonica* were clustered as a single species. In the other two scenarios we split the most widely distributed species into two putative sister species: Split 1 and Split 2. In Split 1 (Figure 2d) *P. pusilla* was divided into two

putative species (*P. pusilla*_west, clustering the samples of the Atlantic region and *P. pusilla*_east, clustering the samples of the Mediterranean region of the distribution range of *P. pusilla*). In Split 2 (Figure 2e) *P. jaenensis* was divided into two putative species (*P. jaenensis*_east, clustering the samples from the Iberian Peninsula and *P. jaenensis*_west, clustering the samples outside the Iberian Peninsula, with the Pyrenees as geographic barrier).

2.6. Test for interspecific hybridization

We used the D-statistic (Green et al., 2010; Durand et al., 2011) to evaluate whether hybridization has occurred between species in *Pyramidula*. Assuming that we have a four taxon tree with topology (((P1, P2), P3), O), under the null hypothesis of no hybridization, the two non-concordant allele patterns (ABBA, where P2 and P3 share the allele B; and BABA, where P1 and P3 share the allele B) are expected to occur with equal frequencies, so that D (the difference between the numbers of ABBA and BABA counts) = 0. Significant deviation of D from 0 rejects the null hypothesis of incomplete lineage sorting, suggesting that hybridization has occurred between P3 and either P1 or P2.

Eaton and Ree (2013) presented an extension of the D-statistic (called "partitioned D-statistic test") which allows for a better detection of interspecific hybridization and enables to infer the directionality of gene flow (i.e. from P2/P1 into P3, from P3 into P1/P2, or in both directions). This partitioned D-statistic is based on a five-taxon tree (((P1, P2), ($P3_1$, $P3_2$)), O), where $P3_1$ and $P3_2$ are two lineages from within the P3 clade. In this case, three D-statistics are estimated: D_1 measures whether the counts non-concordant sites of ABBAA and BABAA are significantly different; D_2 measures whether the counts of ABABA and BAABA are significantly different; and D_12 measures whether the counts of ABBBA and BABBA are significantly different. While D_1 and D_2 reflect the signal of gene flow involving $P3_1$ and $P3_2$ respectively, D_12 reflects interspecific gene flow involving the branch of the most recent common ancestor of $P3_1$ and $P3_2$. D_12 indicates whether gene flow existed from P3 into P1/2, or in the opposite direction: if hybridization occurred from P3 into P1/2, both $P3_1$ and $P3_2$ lineages should share derived alleles resulting in a significant D_12. Conversely, a non-significant D_12 means that gene flow occurred from P1/2 into $P3_1$ or $P3_2$.

In order to evaluate the existence of ancestral hybridization between species in *Pyramidula*, each terminal was selected as follows in the four-taxon D-statistic test: P1

and P2 were two sister species in our trees; P3 was selected as a sister-species of clade P1P2; a different species was used as outgroup (O). Since different individuals can represent the same terminal taxon of P1, P2 and P3, all possible combinations of individuals for a given tree were tested. For those four-taxon D-statistic tests that rejected the null hypothesis of no gene flow, partitioned D-statistic tests were performed in order to infer the directionality of gene flow. Taxa for each terminal were the same as in the four-taxon D-statistic tests but adding two individuals of the same species to P3 ($P3_1$ and $P3_2$). This partitioned D-statistic test was only performed in those cases where two P3 lineages were available.

All tests were performed in *pyRAD* (http://dereneaton.com/software) including heterozygous sites and employing 1000 bootstrap iterations to estimate the value and standard deviation of D. Significance was determined by converting the resultant Z-scores into a two-tailed *P*-value. The standard Bonferroni correction for multiple comparisons was applied.

3. Results

3.1. RADseq data processing

The Illumina MySeq yielded an average of 655,063 reads per sample (first reads) ranging from 292,674 to 1.6 x 10^6. After phred quality filtering, it was reduced to an average of 383,593 reads per sample, ranging from 154,784 to 972,898 (Table 1). The size of the nine *pyRAD* output data matrices and the number of SNPs they included decreased with increasing "minimum depth of coverage" and "similarity threshold" (Figure 3). The length of the matrices of the concatenated sequences ranged from 857,081 to 2,272,846 positions; and the numbers of SNPs ranged from 54,954 to 159,712 (Figure 3).

Taking into account that the length of the nine *pyRAD* output matrices and their content in SNPs varied very little when decreasing the similarity threshold from 90% to 85% (Figure 3), we assumed that decreasing the similarity threshold below 90% was not needed to substantially improve the identification of orthologous loci. Yet, for the "minimum depth of coverage" there were huge differences between tests for the length of matrices and number of SNPs, probably because some of our samples had a very low coverage (e.g. using similarity threshold = 0.90 and minimum taxon coverage = 18, for a minimum depth of coverage = 3 the length of the matrices was 2,305,100 positions

with 156,108 SNPs, while for a minimum depth of coverage = 7 the length of the matrices was 904,462 positions with 59,484 SNPs). We selected a minimum depth of coverage of 5 in order to reduce the chances to include sequencing errors and, at the same time, to include a maximum of loci with a low depth. The "minimum taxon coverage" parameter influenced drastically the length of the matrices, the number of SNPs and missing data obtained with a clustering threshold set to 90% and a minimum depth of coverage set to 5 (2,846,408, 1,459,651 and 415,737 positions, 173,440, 97,269 and 29,079 SNPs and 28.87%, 15.98 and 4.85% missing data, respectively for minimum taxon coverage of 12, 18 and 23).

3.2. Phylogenetic inference

3.2.1. RADseq phylogeny

The eleven RADseq matrices yielded the same tree topology with maximal support for all clades, except for one clade with a bootstrap support value of 95% (Figure 4a).

The nine species delimited by Razkin (2016) received maximal support in the RADseq trees (Figure 4a) and were grouped into two main clades. The first clade included *P. cephalonica, P. chorismenostoma, P. jaenensis, P.* cf. *hierosolymitana, Pyramidula* sp1 and *Pyramidula* sp2, with *P. chorismenostoma* and *P. jaenensis* being sister taxa forming a clade with *P. cephalonica* and *Pyramidula* sp2. The nodes where *P.* cf. *hierosolymitana* and *Pyramidula* sp1 branched off were situated deeper in the tree. The second clade grouped the remaining species, *P. pusilla, P. rupestris* and *P. saxatilis*, with the latter two being sister species.

The two *P.* cf. *cephalonica* individuals (e, f) that showed patterns of incomplete lineage sorting in the study of Razkin et al. (2016) are sister-taxa and as such they clustered with all other *P. cephalonica* specimens.

3.2.2. Five-gene phylogeny

Basic sequence information of these data is provided in Table 2. *P. pusilla, P. rupestris* and *P.* cf. *hierosolymitana* were the only species that were recovered as well-supported clades in each of the three datasets (COI+16S, 5.8S+ITS2+28S, all concatenated) (Figure 4b-d). The monophyly of *P. saxatilis* was supported by the COI+16S and concatenated datasets, whereas the monophyly of *Pyramidula* sp2 was supported by the 5.8S+ITS2+28S and the concatenated datasets. *P. jaenensis* was never supported, but neither rejected, and *Pyramidula* sp2 was not resolved in the COI+16S tree. The

position and monophyly of *P. cephalonica* was ambiguously resolved: in the COI+16S and concatenated trees, *P.* cf. *cephalonica* e-f were grouped together in a clade with *P. jaenensis* and *P. chorismenostoma*. However, in the 5.8S+ITS2+28S tree, *P. cephalonica* a-f formed a well-supported clade. In the three trees *P. cephalonica, P. chorismenostoma, P. jaenensis* and *Pyramidula* sp2 formed a well-supported clade. *P. pusilla, P. rupestris* and *P. saxatilis* were grouped together in the 5.8S+ITS2+28S and concatenated datasets. The three trees strongly supported the sister relationship between *P. rupestris* and *P. saxatilis*. In the 5.8S+ITS2+28S and all concatenated trees *Pyramidula* sp1 grouped with *P. cephalonica, P. chorismenostoma, P. jaenensis* and *Pyramidula* sp2, while in the COI+16S tree *Pyramidula* sp1 was not grouped to any other species being situated deeper in the tree. The positions of *P. jaenensis, Pyramidula* sp2 and *P. chorismenostoma* were not resolved in 5.8S+ITS2+28. The deeper nodes were poorly resolved in COI+16S tree.

3.3. Species delimitation

3.3.1. Species tree

The consensus species tree inferred for the base species delimitation model suggested by Razkin et al. (2016) is shown in Figure 5. This species tree was obtained using 875 unlinked biallelic markers in SNAPP. Relationships between species in the recovered topology were consistent with those estimated using ML of the concatenated rmatrix of RADseq data (Figure 4a), except for the most recent common ancestor of *P. cephalonica*, *Pyramidula* sp2 and *P. chorismenostoma* + *P. jaenensis* that was not recovered (PP = 0.5). For the remaining nodes high PP were found (> 0.99).

3.3.2. Comparisons between species delimitation scenarios

The tested species delimitation models are represented in Figure 2 and the results are summarized in Table 3. The base scenario with nine species (Razkin et al., 2016) was favoured over the alternative delimitation models. The two models clustering closely related species into a single species were consistently rejected. The other two models in which widely distributed species were split into two species were also rejected, although their marginal likelihood values were closer to that of the base scenario.

3.4. Test for intraspecific hybridization

3.4.1. Four-taxon D-statistics test

All D-statistics were based on loci obtained by *pyRAD* using a minimum depth of coverage of 5 and similarity threshold at 90%. Eight D-statistic tests were run for distinct four-taxon subtrees and repeated over all possible combinations of individuals. ummary results are shown in Table 4 and full results of each replicate (unique combinations of individuals) are available in online Supplementary data 3 (awaiting repository number).

We first tested for gene flow between *P. pusilla* and either *P. rupestris* or *P. saxatilis* (test 1). This test found eight significant replicates out of 24 between *P. pusilla* and *P. saxatilis* using a significance level of $\alpha = 0.05$, but one significant replicate out of 24 between the two taxa with a significance level of $\alpha = 0.01$. Tests 2-5 examined whether *P. cephalonica*, *P.* cf. *hierosolymitana*, *Pyramidula* sp1 and *Pyramidula* sp2 hybridized with either *P. chorismenostoma* or *P. jaenensis*. No significant differences were detected in the counts of non-concordant allele patterns in any of the replicates of tests 2 and 3. Tests 4 and 5 provided some significant replicates of gene flow between *P. chorismenostoma* and *Pyramidula* sp1 (test 4: 2 out of 4 with $\alpha = 0.05$), and between *P. chorismenostoma* and *Pyramidula* sp2 (test 5: 2 out of 8 with $\alpha = 0.05$ and 1 out of 8 with $\alpha = 0.01$), respectively. Finally, tests 6-8 explored whether gene flow occurred between *P.* cf. *hierosolymitana* or *Pyramidula* sp1 or *Pyramidula* sp2 and *P. cephalonica* or *P. chorismenostoma*. No significant results were detected for test 7. Tests 6 and 8 provided some significant replicates of gene flow between *P. cephalonica* and *P.* cf. *hierosolymitana* (tests 6: 6 out of 12 with $\alpha = 0.05$ and 1 out of 12 with $\alpha = 0.01$), and between *P. cephalonica* and *Pyramidula* sp2 (test 8: 9 out of 12 with $\alpha = 0.05$ and 1 out of 12 with $\alpha = 0.01$). After Bonferroni correction for multiple comparisons none of the tests remained significant.

3.4.2. Partitioned D-statistics

Partitioned D-statistic tests were only performed for those four-taxon D-statistic tests that showed some signal of ancestral interspecific gene (tests 1, 4, 5, 6 and 8, before Bonferroni correction). Since two different individuals from P3 were needed ($P3_1$ and $P3_2$) test 4 could not be done (Table 5, online Supplementary data 3). Generally more than 100 sites for each allele pattern were obtained for D_12, but fewer than 60 sites for each llele pattern in D_1 and D_2 for all replicates, so reducing their statistical power.

For test 1, D_12 provided the strongest evidence of gene flow between *P. saxatilis* and the most recent common ancestor of *P. pusilla* a-d, since 13 of the 36 replicates were

significant for α = 0.05 and 4 out of 36 for α = 0.01. D_1 was significant for a few replicates suggesting gene flow between both *P. pusilla – P. saxatilis* and *P. pusilla – P. rupestris*. Also D_2 was significant for a few replicates indicating a possible gene flow between *P. pusilla* and *P. rupestris.* Having obtained a significant D_12 (but not being both D_1 and D_2 significant) means that gene flow may have occurred from *P. saxatilis* into both *P. pusilla* lineages selected as $P3_1$ and $P3_2$. Another possible scenario is that the ancestor of the two lineages of *P. pusilla* hybridized with *P. saxatilis.* The significant replicates in D_1 and D_2 indicating a possible gene flow between *P. pusilla* and *P. rupestris* are too weak to take into account since few non-concordant sites were available in D_1 and D_2 tests, and also because none of the four-taxon D-statistic tests found any signal of gene flow between *P. pusilla* and *P. rupestris*. For the remaining tests (5, 6 and 8) very few replicates yielded significant evidence of gene flow between species (Table 5). After Bonferroni correction for multiple comparisons only two replicates from test 1 remained significant (shown in online Supplementary data 3).

4. Discussion

This study provides the very first illustration of jointly applying phylogenetic inference, testing for interspecific hybridization and species delimitation using RADseq data to successfully resolve longstanding taxonomic and phylogenetic problems in a non-model cryptic species complex.

4.1. Phylogenetic inference

The mtDNA (Figure 4c) and nDNA (Figure 4d) trees on their own did not support the nine putative species of *Pyramidula* suggested by Razkin et al. (2016). The combination of mtDNA and nDNA fragments increased support values (Figure 4b), but still some species and interspecific relationships were not fully resolved in the five-genes-trees. The RADseq approach, however, yielded a fully resolved tree (Figure 4a) with (near) maximally supported nodes confirming the monophyly of the nine species suggested by Razkin et al. (2016). The uncertain position of *Pyramidula* sp1 for mtDNA and nDNA gene trees was successfully resolved with the RADseq phylogeny. While the nDNA tree included *Pyramidula* sp1 in the major clade containing *P. pusilla, P. rupestris* and *P. saxatilis*, the tree based on mtDNA fragments did not support its relationships with other species. The RADseq tree included *Pyramidula* sp1 with full support in a different clade clustering *P. cephalonica, P. jaenensis, P. chorismenostoma* and *Pyramidula* sp2. The number of nucleotides in the combined dataset of mtDNA and nDNA was 2,451 bp

with 287 polymorphic sites, whereas the RADseq dataset for the tree construction comprized 1,459,651 bp with 97,269 polymorphic sites; hence, the increased number of markers of the RADseq data helped to fully resolve the phylogenetic relationships between species. This is in line with other recent studies using reduced representation genomic data to resolve phylogenetic relationships among closely related species (Escudero et al., 2014; Hipp et al., 2014; Takahashi et al., 2014).

4.2. Interspecific hybridization

Although interspecific hybridization at various degrees of phylogenetic and taxonomic divergence (even up to generic level) is well documented in terrestrial molluscs (*Cerion*: Galler and Gould, 1979; Woodruff and Gould, 1987; Woodruff, 1989; *Partula*: Johnson et al., 1993; *Cepaea:* Johnson, 1976; *Albinaria*: Schilthuizen and Lombaerts, 1994), our analyses of *Pyramidula* provided only weak (and after Bonferroni correction nearly no) evidence of gene flow between species. The strongest signal of ancestral interspecific hybridization, based on four taxon and partitioned D-statistic tests, was found between *P. pusilla* and *P. saxatilis*. Hybridization implies contact between both species. The distribution of *P. pusilla* is the widest among the studied species and overlaps with the distribution of almost all other species. In addition, the niche modeling analyses of Razkin et al. (2016), suggested that *P. saxatilis* is the only species whose ecological niche model does not significantly differ from that of *P. pusilla*. Besides, the species tree (Figure 5) suggests longer diversification processes in the group of *P. pusilla*, *P. saxatilis* and *P. rupestris* than in the remaining species. Thus, *P. pusilla* and *P. saxatilis* may have shared the same niche in the same area at some time, making admixture possible. Indeed, other studies on land snails have suggested hybridization at occasional contact zones or following diversification events (Douris et al., 2007).

The partitioned D-test provided no conclusive evidence with respect to the directionality of eventual gene flow between *P. pusilla* and *P. saxatilis*. Replicates of test 1 in which D_12 yielded significant differences in non-concordant allele patterns suggested gene flow between *P. pusilla* and *P. saxatilis*. However, in these replicates, the test did not find any significant D_1 and D_2. These results can be explained by two different scenarios. The first one is that the direction of gene flow occurred from *P. pusilla* into *P. saxatilis*: the ancestor of the two *P. pusilla* lineages, or a lineage which diverged from this ancestor, could introgress into *P. saxatilis*. The alternative scenario is that gene flow

passed from *P. saxatilis* into both *P. pusilla* lineages. Therefore, we cannot conclude in which direction eventual gene flow occurred.

The remaining species showed non-significant or very weak signals of ancestral interspecific gene flow and therefore, incomplete lineage sorting may explain the differences in the non-concordant allele patterns. The species tree (Figure 5) suggests that *P. cephalonica, P. chorismenostoma* and *P. jaenensis* underwent more rapid radiations, being hence good candidates for incomplete lineage sorting (Whitfield and Lockhart, 2007).

4.3. Species delimitation

Razkin et al. (2016) suggested nine putative species in the *Pyramidula* species complex in Europe, based on an integrative species delimitation approach using molecular (mtDNA COI and 16S and nuclear 5.8S-ITS2-28S gene fragments) and ecological niche modeling data. We tested four species delimitation scenarios using RADseq data and Bayes factor delimitation. These results confirmed that the base scenario of 9 putative species was the most plausible one. The four alternative scenarios included two clustering and two split scenarios. The marginal likelihood values obtained by the two split scenarios were close to the best scenario (base scenario). One explanation could be that arbitrarily splitting species is the most difficult scenario to distinguish from the true model if split populations are connected by low gene flow (Leaché et al., 2014).

In both, the present study and the study of Razkin et al. (2016), the procedure of species delimitation required the construction of a species tree. Razkin et al. (2016) constructed the species tree for the dataset of five genes using *BEAST implemented in BEAST v 1.8 (Drummond and Rambaut, 2007). This Bayesian method for tracing multispecies coalescense coestimates multiple gene trees embedded in a shared species tree (Heled and Drummond, 2010). Several nodes in the species tree obtained in Razkin et al. (2016) were not supported. In contrast, in the present study the species tree was inferred in SNAPP (Bryant et al., 2012). This method estimates the likelihood of species tree topology also based on a multispecies coalescent model, but using unlinked biallelic markers instead of sampling gene trees. The resulting species tree recovered all nodes with high posterior supports (> 0.99), except for the clustering of *P. cephalonica, P. chorismenostoma* and *P. jaenensis*. As suggested above, these species could have undergone a rapid radiation and hence, their phylogenetic relationships can be more difficult to resolve. The remaining part of the tree topology was fully supported, making

its resolution more complete than that obtained using five gene fragments in Razkin et al. (2016). The topology obtained in the species tree supported the results of the phylogenetic inference on the concatenated RADseq dataset. These results demonstrated the benefit of using potentially unlinked markers to reconstruct a species tree. Since analyzing a large number of gene trees under the coalescent model is computationally challenging, using multiple unlinked biallelic markers becomes a feasible alternative to infer species trees.

4.4. Implications for *Pyramidula*

RADseq resolved taxonomic issues for a cryptic species complex of the land snail *Pyramidula* that were undecided in the approach of Razkin et al. (2016) using morphological, niche modeling and DNA data. Analyzing mtDNA and nDNA trees separately enabled inspecting incongruence patterns. While the nDNA tree grouped all *P. cephalonica* samples (a-f) together, the mtDNA tree grouped *P. cephalonica* a-d samples and *P.* cf. *cephalonica* e-f samples separately. Although not supported (nor contradicted) in the mtDNA tree of the present study, the grouping of *P.* cf. *cephalonica* e-f with *P. chorismenostoma* was supported in the mtDNA tree of Razkin et al. (2016) (where more samples of both *P.* cf. *cephalonica* and *P. chorismenostoma* could be included). This incongruence between nDNA and mtDNA phylogenies, together with the distribution and morphology of the analyzed samples suggested the possibility of interspecific gene flow between *P. cephalonica* and *P. chorismenostoma*, or incomplete lineage sorting. The phylogenetic RADseq trees fully supported the grouping of all *P. cephalonica* samples (a-f) and, taking into account that the morphology and distribution of *P.* cf. *cephalonica* e-f concur with that of *P. cephalonica* a-d, we conclude that *P.* cf. *cephalonica* e-f and *P. cephalonica* a-d are conspecific. Interspecific hybridization tests did not find significant signals of ancestral interspecific gene flow between *P. cephalonica* and *P. chorismenostma*. Besides, branch lengths of the species tree suggested that the clade clustering *P. cephalonica*, *P. chorismenostoma* and *P. jaenensis* underwent rapid radiations, making their admixture more difficult. Gene flow levels are higher in those areas where species live in sympatry (Ballard and Whitlock, 2004) but in this case the samples analyzed of *P.* cf. *cephalonica* e-f and *P. chorismenostoma* were not sympatric, making the hypothesis of recent hybridization less plausible. All these information jointly suggested that incongruence between the mtDNA and nDNA gene trees regarding *P. cephalonica* and *P. chorismenostoma* may be due to incomplete

lineage sorting of the mtDNA, due to a rapid speciation process (Avise, 2000). Incomplete lineage sorting has also been effectively documented in other molluscs (Periwinkles: Wilding et al. 2000; *Oncomelaria hupensis:* Wilke et al. 2005; pyrgulinid microgastropods: Schreiber et al. 2011). Although some shell characters could discriminate between some of the species in *Pyramidula*, they are not able to differentiate all of them, and hence, they are not valid as unique taxonomic criteria (Razkin et al., 2016). Particularly *P. pusilla* and *P. saxatilis* cannot be distinguished based on the relative height of the shell (height/diameter). Therefore, shell morphology would not be useful to infer interspecific gene flow between both species.

Two decades after Gittenberger and Bank (1996) defined the morphological species of *Pyramidula* in Europe splitting *Pyramidula rupestris* on conchological basis, the present study provides the phylogenetic basis and framework of these species using high throughput sequencing. Combining the present work and the study of Razkin et al. (2016) we conclude that the shell characters used until now to define *Pyramidula* species are not reliable (height, maximum diameter and umbilicus diameter). The use of mitochondrial genes (COI+16S) is enough to identify the European species *P. pusilla*, *P. rupestris*, *P. saxatilis* and *P. jaenensis.* Mitochondrial phylogenies may group together *P. cephalonica* and *P. chorismenostoma* due to incomplete lineage sorting, but the conspicuous scalarid shell of *P. chorismenostoma* (body whorl separated from the rest of the shell) distinguishes both species. A similar study including samples from Asia is needed to elucidate the taxonomy of the remaining *Pyramidula* species. A similar study including samples from Asia is needed to elucidate the taxonomy of the remaining *Pyramidula* species.

Supplementary material:

Supplementary material can be found at http://datadryad.org in the Dryad data repository X (awaiting repository number).

Acknowledgements:

This paper was produced in the context of the BELSPO IUAP project "SPEEDY" and the FWO (Flanders) research community W0.009.11N "Belgian Network for DNA Barcoding". It was partially funded by the Basque Government through the Research

group on “Systematics, Biogeography and Population Dynamics” (IT575-13). O. Razkin obtained the PhD funding of the Department of Education of the Government of Navarra and a travel grant of the University of the Basque Country (UPV/EHU). We are grateful to Carl Vangestel (RBINS) and Frederik Hendrickx (RBINS) for the help provided in the RADseq library preparation process.

References

Avise, J.C., 2000. Phylogeography: The history and formation of species. Harvard University Press, Cambridge, MA.

Baird, N.A., Etter, P.D., Atwood, T.S., Currey, M.C., Shiver, A.L., Lewis, Z.A., Selker, E.U., Cresko, W.A., Johnson, E.A., 2008. Rapid SNP discovery and genetic mapping using sequenced RAD markers. PLoS One 3, e3376. doi:10.1371/journal.pone.0003376

Ballard, J.W.O., Whitlock, M.C., 2004. The incomplete natural history of mitochondria. Mol. Ecol. 13, 729–744. doi:10.1046/j.1365-294X.2003.02063.x

Bouckaert, R., Heled, J., Kühnert, D., Vaughan, T., Wu, C.-H., Xie, D., Suchard, M.A., Rambaut, A., Drummond, A.J., 2014. BEAST 2: a software platform for Bayesian evolutionary analysis. PLoS Comput. Biol. 10, e1003537. doi:10.1371/journal.pcbi.1003537

Bryant, D., Bouckaert, R., Felsenstein, J., Rosenberg, N.A., RoyChoudhury, A., 2012. Inferring species trees directly from biallelic genetic markers: bypassing gene trees in a full coalescent analysis. Mol. Biol. Evol. 29, 1917–1932. doi:10.1093/molbev/mss086

Catchen, J., Hohenlohe, P.A., Bassham, S., Amores, A., Cresko, W.A., 2013. Stacks: an analysis tool set for population genomics. Mol. Ecol. 22, 3124–3140. doi:10.1111/mec.12354

Catchen, J.M., Amores, A., Hohenlohe, P., Cresko, W., Postlethwait, J.H., 2011. Stacks: building and genotyping loci de novo from short-read sequences. G3 (Bethesda) 1, 171–182. doi:10.1534/g3.111.000240

Davey, J.L., Blaxter, M.W., 2010. RADSeq: next-generation population genetics. Brief. Funct. Genom. 9, 416–423. doi:10.1093/bfgp/elq031

Degnan, J.H., Rosenberg, N.A., 2009. Gene tree discordance, phylogenetic inference and the multispecies coalescent. Trends Ecol. Evol. 24, 332–340. doi:10.1016/j.tree.2009.01.009

Douris, V., Giokas, S., Thomaz, D., Lecanidou, R., Rodakis, G.C., 2007. Inference of evolutionary patterns of the land snail *Albinaria* in the Aegean archipelago: is vicariance enough? Mol. Phylogenet. Evol. 44, 1224–1236. doi:10.1016/j.ympev.2007.01.004

Drummond, A.J., Rambaut, A., 2007. BEAST: Bayesian evolutionary analysis by sampling trees. BMC Evol. Biol. 7, 214. doi:10.1186/1471-2148-7-214

Durand, E.Y., Patterson, N., Reich, D., Slatkin, M., 2011. Testing for ancient admixture between closely related populations. Mol. Biol. Evol. 28, 2239–2252. doi:10.1093/molbev/msr048

Eaton, D.A.R., 2014. PyRAD: assembly of de novo RADseq loci for phylogenetic analyses. Bioinformatics 1–6. doi:10.1093/bioinformatics/btu121

Eaton, D.A.R., Ree, R.H., 2013. Inferring phylogeny and introgression using RADseq data: an example from flowering plants (*Pedicularis*: Orobanchaceae). Syst. Biol. 62, 689–706. doi:10.1093/sysbio/syt032

Edgar, R.C., 2004. MUSCLE: multiple sequence alignment with high accuracy and high throughput. Nucleic Acids Res. 32, 1792–1797. doi:10.1093/nar/gkh340

Emerson, K.J., Merz, C.R., Catchen, J.M., Hohenlohe, P.A., Cresko, W.A., Bradshaw, W.E., Holzapfel, C.M., 2010. Resolving postglacial phylogeography using high-throughput sequencing. Proc. Natl. Acad. Sci. USA 107, 16196–16200. doi:10.1073/pnas.1006538107

Escudero, M., Eaton, D.A.R., Hahn, M., Hipp, A.L., 2014. Genotyping-By-Sequencing as a tool to infer phylogeny and ancestral hybridization: A case study in *Carex* (Cyperaceae). Mol. Phylogenet. Evol. 79, 359–367. doi:10.1016/j.ympev.2014.06.026

Etter, P.D., Preston, J.L., Bassham, S., Cresko, W.A., Johnson, E.A., 2011. Local de novo assembly of RAD paired-end contigs using short sequencing reads. PLoS One 6, e18561. doi:10.1371/journal.pone.0018561

Galler, L., Gould, S.J., 1979. The morphology of a “hybrid zone” in *Cerion*: Variation, clines, and an ontogenetic relationship between two “species” in Cuba. Evolution 33, 714–727.

Gittenberger, E., Bank, R., 1996. A new start in *Pyramidula* (Gastropoda Pulmonata: Pyramidulidae). Basteria 60, 71–78.

Goodfriend, G.A., 1986. Variation in land-snail shell form and size and its causes: a review. Syst. Biol. 35, 204–223. doi:10.1093/sysbio/35.2.204

Green, R.E., Krause, J., Briggs, A.W., Maricic, T., Stenzel, U., Kircher, M., Patterson, N., Li, H., Zhai, W., Fritz, M.H.-Y., Hansen, N.F., Durand, E.Y., Malaspinas, A.-S., Jensen, J.D., Marques-Bonet, T., Alkan, C., Prüfer, K., Meyer, M., Burbano, H.A., Good, J.M., Schultz, R., Aximu-Petri, A., Butthof, A., Höber, B., Höffner, B., Siegemund, M., Weihmann, A., Nusbaum, C., Lander, E.S., Russ, C., Novod, N., Affourtit, J., Egholm, M., Verna, C., Rudan, P., Brajkovic, D., Kucan, Z., Gusic, I., Doronichev, V.B., Golovanova, L. V, Lalueza-Fox, C., de la Rasilla, M., Fortea, J., Rosas, A., Schmitz, R.W., Johnson, P.L.F., Eichler, E.E., Falush, D., Birney, E., Mullikin, J.C., Slatkin, M., Nielsen, R., Kelso, J., Lachmann, M., Reich, D., Pääbo, S., 2010. A draft sequence of the Neandertal genome. Science 328, 710–722. doi:10.1126/science.1188021

Gómez-Moliner, B.J., 1988. Estudio sistemático y biogeográfico de los moluscos terrestres del Suborden Orthurethra (Gastropoda: Pulmonata: Stylommatophora) del País Vasco y regiones adyacentes, y catálogo de las especies ibéricas. Ph.D. Thesis. Universidad del País Vasco, Spain.

Harley, C.D.G., Denny, M.W., Mach, K.J., Miller, L.P., 2009. Thermal stress and morphological adaptations in limpets. Funct. Ecol. 23, 292–301. doi:10.1111/j.1365-2435.2008.01496.x

Heled, J., Drummond, A.J., 2010. Bayesian inference of species trees from multilocus data. Mol. Biol. Evol. 27, 570–580. doi:10.1093/molbev/msp274

Heller, J., 1987. Shell shape and land-snail habitat in a Mediterranean and desert fauna. Biol. J. Linn. Soc. 31, 257–272. doi:10.1111/j.1095-8312.1987.tb01992.x

Hipp, A.L., Eaton, D.A.R., Cavender-Bares, J., Fitzek, E., Nipper, R., Manos, P.S., 2014. A framework phylogeny of the American oak clade based on sequenced RAD data. PLoS One 9, e93975. doi:10.1371/journal.pone.0093975

Johnson, M.S., 1976. Allozymes and area effects in *Cepaea nemoralis* on the western Berkshire Downs. Heredity 36, 105–121.

Johnson, M.S., Murray, J., Clarke, B., 1993. The ecological genetics and adaptive radiation of *Partula* on Moorea. Oxford Surv. Evol. Biol. 9, 167–238.

Katoh, K., Standley, D.M., 2013. MAFFT multiple sequence alignment software version 7: improvements in performance and usability. Mol. Biol. Evol. 30, 772–780. doi:10.1093/molbev/mst010

Katoh, K., Toh, H., 2008. Improved accuracy of multiple ncRNA alignment by incorporating structural information into a MAFFT-based framework. BMC Bioinformatics 9, 212. doi:10.1186/1471-2105-9-212

Kerney, M., 1999. Atlas of the land and freshwater molluscs of Britain and Ireland. Harley Books, Colchester.

Kubatko, L.S., 2009. Identifying hybridization events in the presence of coalescence via model selection. Syst. Biol. 58, 478–488. doi:10.1093/sysbio/syp055

Leaché, A.D., Fujita, M.K., Minin, V.N., Bouckaert, R.R., 2014. Species delimitation using genome-wide SNP data. Syst. Biol. 63, 534–542. doi:10.1093/sysbio/syu018

Librado, P., Rozas, J., 2009. DnaSP v5: a software for comprehensive analysis of DNA polymorphism data. Bioinformatics 25, 1451–1452. doi:10.1093/bioinformatics/btp187

Maddison, W.P., 1997. Gene trees in species trees. Syst. Biol. 46, 523–536. doi:10.1093/sysbio/46.3.523

Maddison, W.P., Knowles, L.L., 2006. Inferring phylogeny despite incomplete lineage sorting. Syst. Biol. 55, 21–30. doi:10.1080/10635150500354928

Martínez-Ortí, A., Gómez-Moliner, B.J., Prieto, C.E., 2007. El género *Pyramidula* Fitzinger 1833 (Gastropoda, Pulmonata) en la Península Ibérica. Iberus 25, 77–87.

Miller, M.A., Pfeiffer, W., Schwartz, T., 2010. Creating the CIPRES Science Gateway for inference of large phylogenetic trees, in: 2010 Gateway Computing Environments Workshop (GCE). IEEE, pp. 1–8. doi:10.1109/GCE.2010.5676129

Razkin, O., Gómez-Moliner, B.J., Vardinoyannis, K., Martínez-Ortí, A., Madeira, M.J., 2016. Species delimitation for cryptic species complexes: case study of *Pyramidula* (Gastropoda, Pulmonata). Zoologica Scripta (in press).

Schileyko, A.A., Balashov, I.A., 2012. *Pyramidula kuznetsovi* sp. nov. – a new species of land molluscs from Nepal (Pulmonata, Pyramidulidae). Ruthenica 22, 41-45.

Schilthuizen, M., Lombaerts, M., 1994. Population Structure and Levels of Gene Flow in the Mediterranean Land Snail *Albinaria corrugata* (Pulmonata: Clausiliidae). Evolution 48, 577–586.

Schlötterer, C., 2004. The evolution of molecular markers--just a matter of fashion? Nature Rev. Genet. 5, 63–9. doi:10.1038/nrg1249

Schreiber, K., Hauffe, T., Albrecht, C., Wilke, T., 2011. The role of barriers and gradients in differentiation processes of pyrgulinid microgastropods of Lake Ohrid. Hydrobiologia 682, 61–73. doi:10.1007/s10750-011-0864-4

Stamatakis, A., 2014. RAxML version 8: a tool for phylogenetic analysis and post-analysis of large phylogenies. Bioinformatics 30, 1312–1313. doi:10.1093/bioinformatics/btu033

Stankowski, S., 2011. Extreme, continuous variation in an island snail: local diversification and association of shell form with the current environment. Biol. J. Linn. Soc. 104, 756–769. doi:10.1111/j.1095-8312.2011.01748.x

Takahashi, T., Nagata, N., Sota, T., 2014. Application of RAD-based phylogenetics to complex relationships among variously related taxa in a species flock. Mol. Phylogenet. Evol. 80, 137–144. doi:10.1016/j.ympev.2014.07.016

Thomson, R.C., Shedlock, A.M., Edwards, S. V, Shaffer, H.B., 2008. Developing markers for multilocus phylogenetics in non-model organisms: A test case with turtles. Mol. Phylogenet. Evol. 49, 514–525. doi:10.1016/j.ympev.2008.08.006

Twyford, A.D., Ennos, R.A., 2011. Next-generation hybridization and introgression. Heredity 108, 179–189. doi:10.1038/hdy.2011.68

Viricel, A., Pante, E., Dabin, W., Simon-Bouhet, B., 2014. Applicability of RAD-tag genotyping for interfamilial comparisons: empirical data from two cetaceans. Mol. Ecol. Resour. 14, 597–605. doi:10.1111/1755-0998.12206

Wagner, C.E., Keller, I., Wittwer, S., Selz, O.M., Mwaiko, S., Greuter, L., Sivasundar, A., Seehausen, O., 2013. Genome-wide RAD sequence data provide unprecedented resolution of species boundaries and relationships in the Lake Victoria cichlid adaptive radiation. Mol. Ecol. 22, 787–798. doi:10.1111/mec.12023

Welter-Schultes, F., 2012. Species summary for *Pyramidula*. Available via www.animalbase.uni-goettingen.de (version 29-11-2012)

Wendel, J.F., Doyle, J.J., 1998. Phylogenetic incongruence: window into genome history and molecular evolution. Mol. Syst. Plants II 265–296.

Whitfield, J.B., Lockhart, P.J., 2007. Deciphering ancient rapid radiations. Trends Ecol. Evol. 22, 258–265. doi:10.1016/j.tree.2007.01.012

Wilding, C.S., Grahame, J., Mill, P.J., 2000. Mitochondrial DNA CoI haplotype variation in sibling species of rough periwinkles. Heredity 85, 62-74.

Wilke, T., Davis, G.M., Qiu, D., Spear, R.C., 2005. Extreme mitochondrial sequence diversity in the intermediate schistosomiasis host *Oncomelania hupensis robertsoni*: another case of ancestral polymorphism? Malacologia 48, 143–157.

Woodruff, D.S., 1989. Genetic anomalies associated with *Cerion* hybrid zones: the origin and maintenance of new electromorphic variants called hybrizymes. Biol. J. Linn. Soc. 36, 281–294. doi:10.1111/j.1095-8312.1989.tb00495.x

Woodruff, D.S., Gould, S.J., 1987. Fifty years of interspecific hybridization: genetics and morphometrics of a controlled experiment on the land snail *Cerion* in the Florida Keys. Evolution 41, 1022–1045.

Yu, Y., Than, C., Degnan, J.H., Nakhleh, L., 2011. Coalescent histories on phylogenetic networks and detection of hybridization despite incomplete lineage sorting. Syst. Biol. 60, 138–149. doi:10.1093/sysbio/syq084

Legends:

Figure 1: Geographic origins of the samples of *Pyramidula*. Stars refer to the samples analyzed using RADseq data in the present study. Dots refer to samples analyzed in Razkin et al. (2016) and provide a rough idea of the distribution of each species.

Table 1: Information on the specimens used in this study, on the RAD tags sequenced here and the Genbank accession numbers from Razkin et al. (2016): RAD tags: reads that passed quality filtering; cluster: number of clusters at 90% similarity; mean depth: mean depth of clusters with depth of coverage ≥ 5; consensus loci: number of loci with depth ≥ 5 and passed paralog filter; loci in final dataset: number of loci available for 18 taxa or more.

Figure 2: (a) Base species delimitation model and (b-e) alternative species delimitation models: (b) Clustering 1: *P. rupestris* + *P. saxatilis*; (c) Clustering 2: *P. jaenensis* + *P. chorismenostoma* + *P. cephalonica*. (d) Split 1: *P. pusilla* = *P. pusilla*_west + *P. pusilla*_east; and (e) Split 2: *P. jaenensis* = *P. jaenensis*_west + *P. jaenensis*_east. Circles refer to approximate distribution areas of species and colors of each species are defined at the top right.

Figure 3: Length of the concatenated sequence dataset (a) and total number of single nucleotide polymorphisms (SNPs) (b) resulting from nine pyRAD analyses where three clustering similarity thresholds and three minimum depth of coverages ('m') were applied. Other two pyRAD analyses are also represented where two different minimum taxon coverage values ('t') were applied.

Figure 4: Phylogenetic trees inferred by maximum-likelihood analyses of: (a) the RADseq supermatrix using clustering threshold = 90%, minimum depth coverage = 5 and minimum taxon coverage = 18. (b) the concatenated mtDNA (COI + 16S) and nDNA (5.8S + ITS2 + 28S) sequences. (c) the concatenated mtDNA sequences. (d) the concatenated nDNA sequences.

Table 2: Sequence lengths and numbers of variable sites of COI, 16S, 5.8S-ITS2, 28S and the combined datasets.

Figure 5: Densitree diagram representing all species trees obtained from SNAPP (left) and consensus topology with posterior probability values (right).

Table 3: Results for BFD* species delimitation: ML (marginal likelihood); BF (Bayes factor).

Table 4: Results of the four taxon D-statistic tests showing the range of Z-scores ("Range *Z*"); number of significant replicates ("Nsig/n"); main allele pattern in significant replicates ("Allele pattern (sigD)"); species involved in introgression; range of number of available RAD loci ("Range nloci"); and range of percentage of non concordant sites over all possible replicates ("Range pdisc").

Table 5: Results of the partitioned D-statistic tests showing the range of Z-scores ("Range Z"); number of significant replicates ("Nsig/n"); main allele pattern in significant replicates ("Allele pattern (sigD)"); range of number of available RAD loci ("Range nloci"); and range of percentage of non concordant sites over all possible replicates ("Range pdisc").

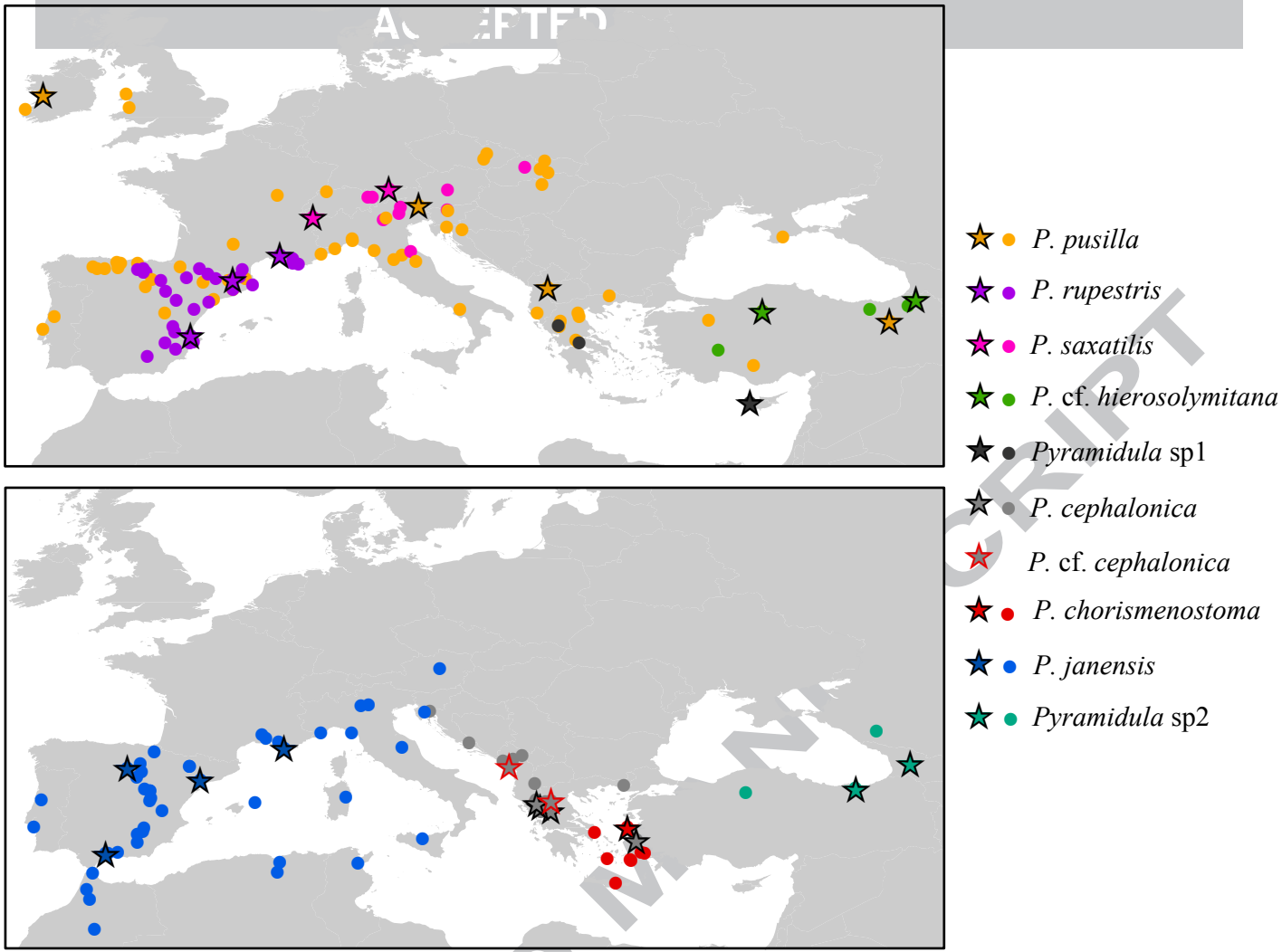
P. pusilla
P. rupestris
P. saxatilis
P. cf. hierosolymitana
Pyramidula sp1
P. cephalonica
P. cf. cephalonica
P. chorismenostoma
P. janensis
Pyramidula sp2

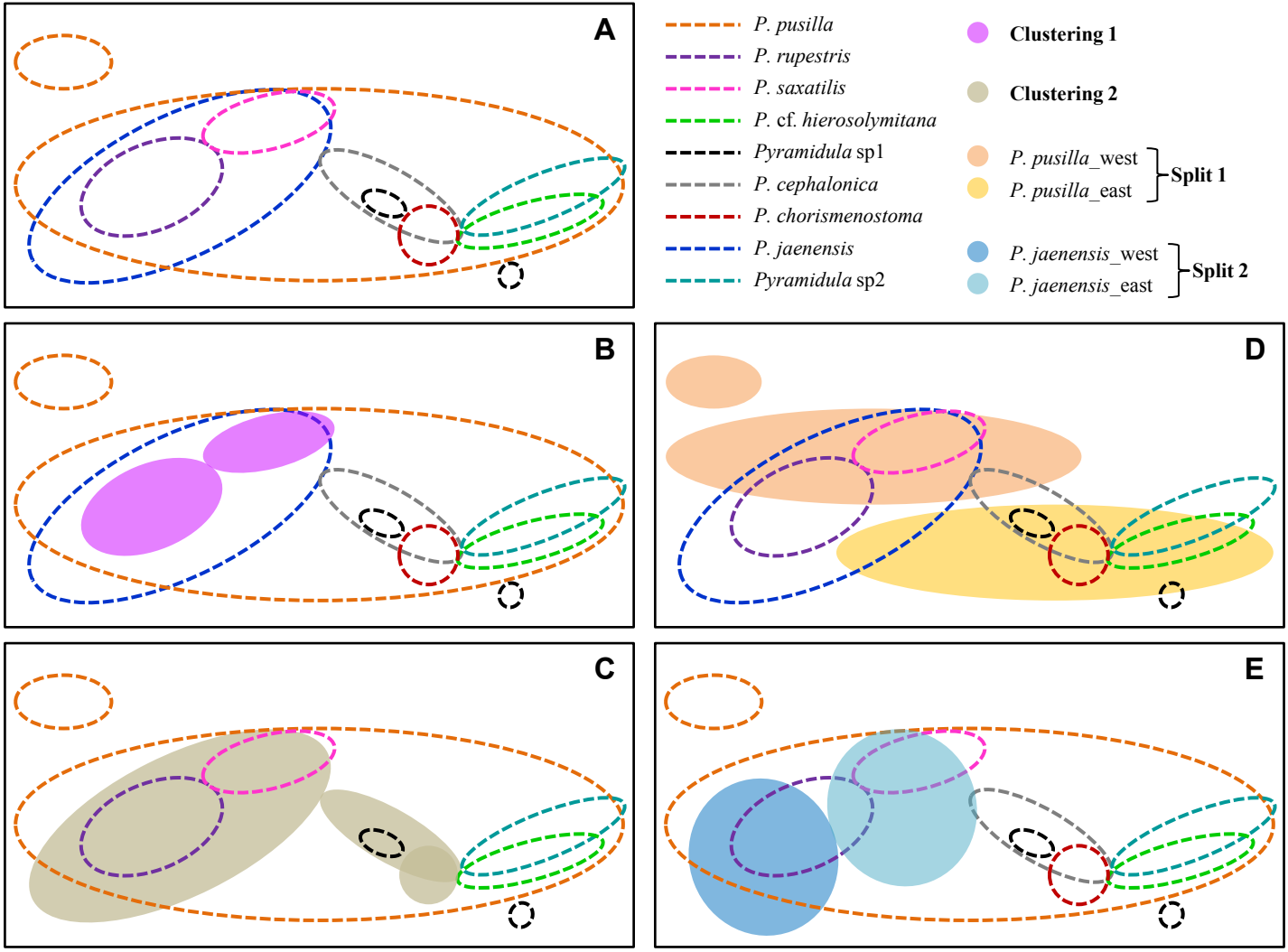
A
B
C
D
E
P. pusilla
P. rupestris
P. saxatilis
P. cf. hierosolymitana
Pyramidula sp1
P. cephalonica
P. chorismenostoma
P. jaenensis
Pyramidula sp2
Clustering 1
Clustering 2
P. pusilla_west
P. pusilla_east
Split 1
P. jaenensis_west
P. jaenensis_east
Split 2

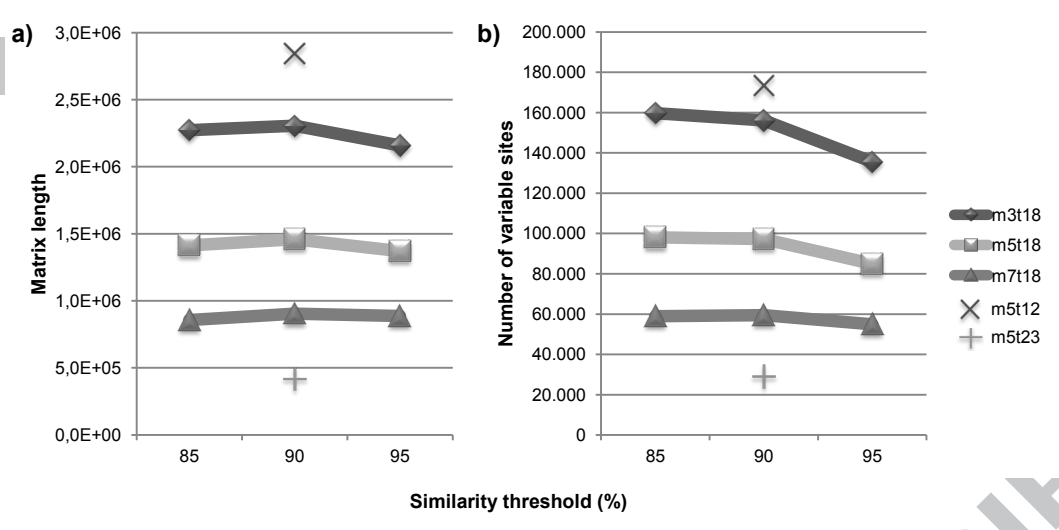
a)
3,0E+06
2,5E+06
2,0E+06
1,5E+06
1,0E+06
5,0E+05
0,0E+00
Matrix length
85
90
95
b)
200.000
180.000
160.000
140.000
120.000
100.000
80.000
60.000
40.000
20.000
0
Number of variable sites
85
90
95
m3t18
m5t18
m7t18
m5t12
m5t23
Similarity threshold (%)

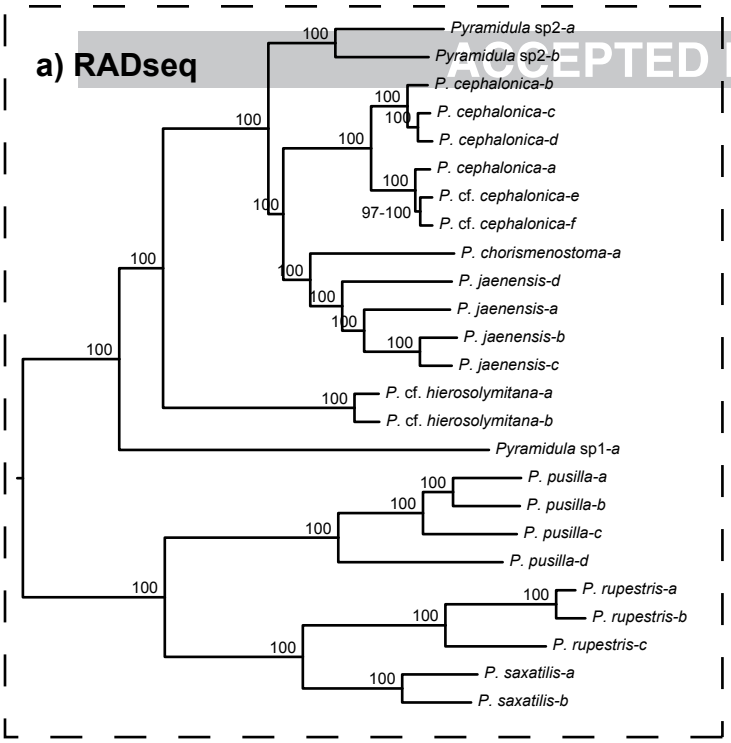

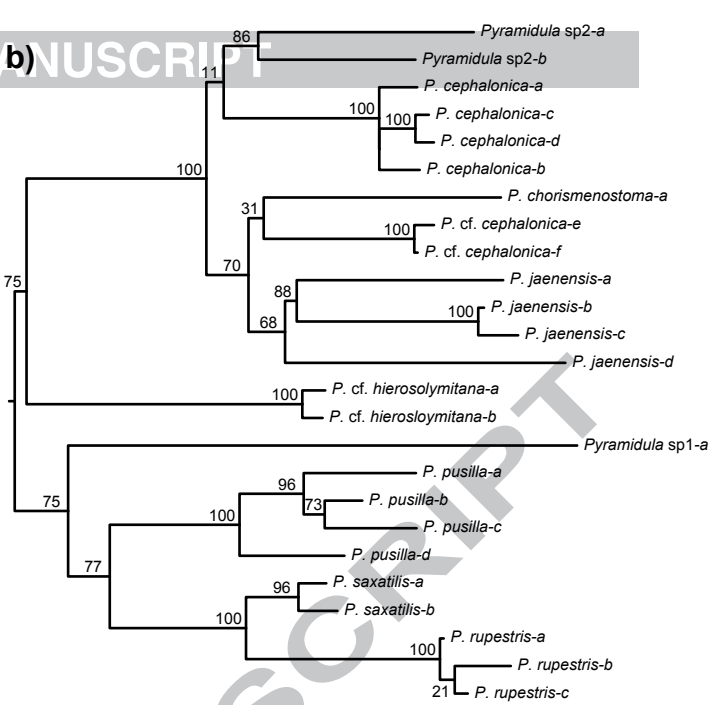

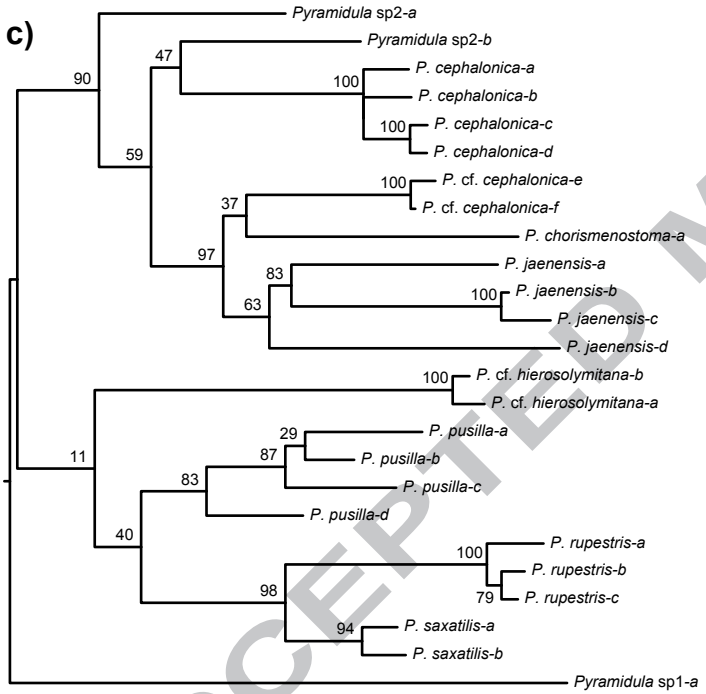

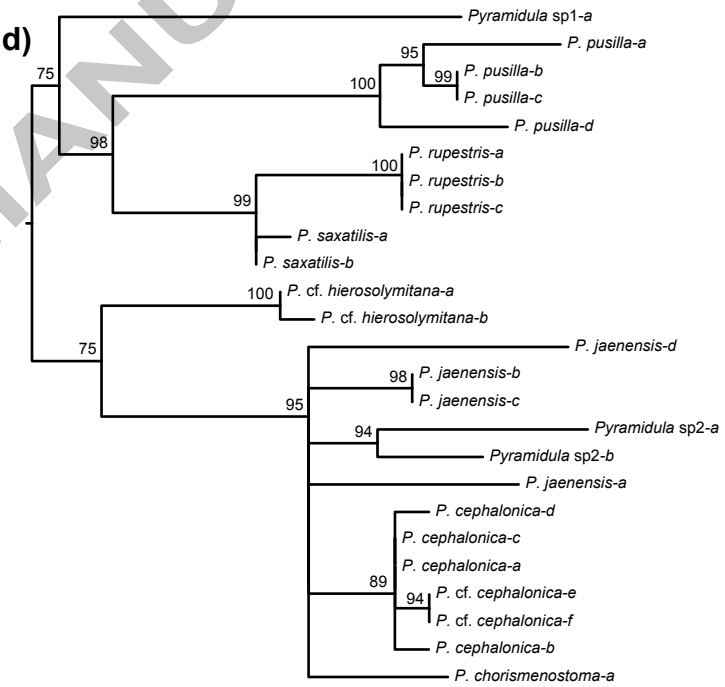

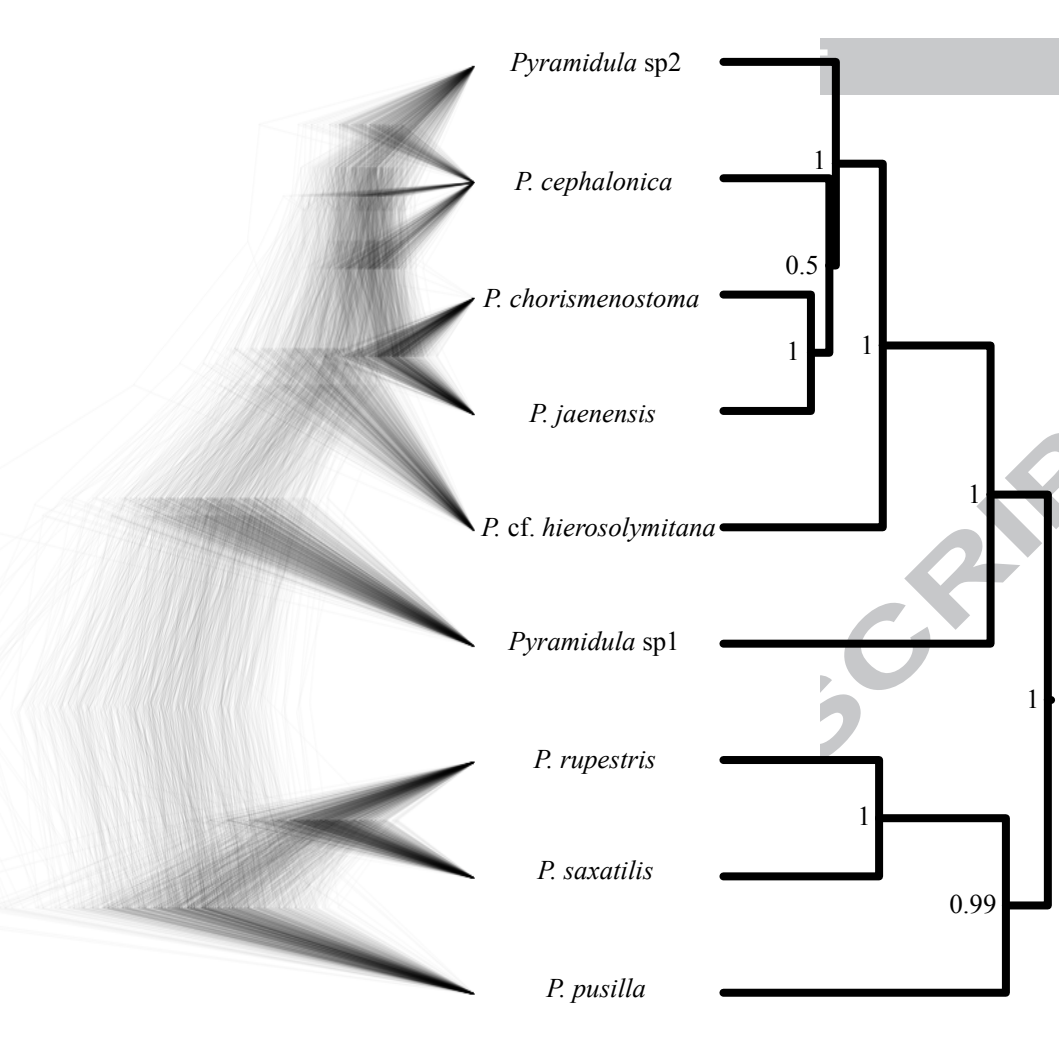
Pyramidula sp2
P. cephalonica
P. chorismenostoma
P. jaenensis
P. cf. *hierosolymitana*
Pyramidula sp1
P. rupestris
P. saxatilis
P. pusilla
1
0.5
1
1
1
1
1
0.99

Voucher number	Species	Locality	RAD tags	Clusters	Mean depth	Consensus loci	Loci in final data set	Genbank COI	Genbank 16S	Genbank nuclear
EHUMC_1201	*P. pusilla*-a	Near Lesachtal, Kärnten, Austria	302,136	38,308	11.428	15,021	4,856	KP727247	KP727036	KP727460
HNHM_99350	*P. pusilla*-b	Korab Mts, Diber, Albania	360,865	58,723	11.378	16,209	5,074	KP727290	KP727079	KP727503
EHUMC_1208	*P. pusilla*-c	Vallyvaughan, Clare, Ireland	380,449	39,592	13.927	14,612	5,097	KP727293	KP727082	KP727506
HNHM_98875	*P. pusilla*-d	Erzurum, Turkey	284,484	40,553	10.803	13,746	4,714	KP727354	KP727143	KP727567
EHUMC_1138	*P. rupestris*-a	Arles, Provence, France	429,798	35,144	15.229	18,796	5,512	KP727157	KP726946	KP727370
MVHN_070910RU15	*P. rupestris*-b	Bellús, Valencia, Spain	307,041	31,028	12.357	15,895	5,198	KP727176	KP726965	KP727389
EHUMC_1225	*P. rupestris*-c	Lillet-Castellar d'Nug, Barcelona, Spain	414,475	30,865	16.005	15,559	5,420	KP727319	KP727108	KP727532
EHUMC_1170	*P. saxatilis*-a	The Alps, France	325,337	35,566	13.119	13,861	5,096	KP727207	KP726996	KP727420
EHUMC_1220	*P. saxatilis*-b	Eschenlohe-Oberau, Bayern, Germany	790,027	131,046	17.181	23,306	5,631	KP727314	KP727103	KP727527
EHUMC_1149	*P.* cf. *hieroslymitana*-a	Artvin, Turkey	410,993	29,065	15.458	15,622	5,514	KP727185	KP726974	KP727398
HNHM_98874_2	*P.* cf. *hieroslymitana*-b	Gümüshane, Turkey	287,216	30,419	12.592	11,972	4,956	KP727353	KP727142	KP727566
NHMC_50.23326_1	*Pyramidula* sp1-a	Petratis gorge, Cyprus	182,297	32,269	9.143	9,275	3,557	KP727277	KP727066	KP727490
EHUMC_1133	*P. jaenensis*-a	Marsella - Toulon, Var, France	500,246	34,469	16.756	19,860	5,817	KP727152	KP726941	KP727365
EHUMC_1140	*P. jaenensis*-b	Valle de Abdalajis, Málaga, Spain	201,257	28,041	10.591	9,576	4,260	KP727159	KP726948	KP727372
EHUMC_1184	*P. jaenensis*-c	Sto Domingo de Silos, Burgos, Spain	247,143	22,880	12.373	11,054	4,817	KP727230	KP727019	KP727443
EHUMC_1227	*P. jaenensis*-d	Codolar, Tarragona, Spain	278,517	35,283	12	12,119	4,937	KP727321	KP727110	KP727534
NHMC_50.27302	*P. chorismenostoma*-a	Chios island, Greece	154,784	31,131	8.937	6,917	3,035	KP727257	KP727046	KP727470
ZMH_86507/999 _2	*Pyramidula* sp 2-a	Imereti, Kutaisi, Georgia	425,231	45,050	14.413	16,546	5,497	KP727331	KP727120	KP727544
HNHM_98871	*Pyramidula* sp 2-b	Trabzon, Turkey	391,970	48,616	14.165	14,947	5,457	KP727349	KP727138	KP727562
NHMC_50.32106_2	*P. cephalonica*-a	Samos island, Greece	315,065	62,779	10.791	12,441	4,828	KP727267	KP727056	KP727480
HNHM_98853_1	*P. cephalonica*-b	Thessaly, Trikala, Greece	478,386	36,531	16.899	16,731	5,815	KP727335	KP727124	KP727548
HNHM_98858	*P. cephalonica*-c	Epirus, Ioannina, Greece	454,324	41,254	15.086	19,090	5,854	KP727341	KP727130	KP727554
HNHM_98859_2	*P. cephalonica*-d	Epirus, Ioannina, Greece	972,898	62,153	26.331	24,097	5,937	KP727343	KP727132	KP727556
HNHM_99349	*P.* cf. *cephalonica*-e	Rumija Mts. Near Stari Bar, Montenegro	285,760	29,683	11.528	15,392	5,466	KP727288	KP727077	KP727501
HNHM_98861	*P.* cf. *cephalonica*-f	Epirus, Ioannina, Greece	409,134	39,985	15.315	14,814	5,586	KP727345	KP727134	KP727558

Table 1: Information on the specimens used in this study, on the RAD tags sequenced here and the Genbank accession numbers from Razkin et al. (under review): RAD tags: reads that passed quality filtering; Cluster: number of clusters at 90% similarity; Mean Depth: mean depth of clusters with depth of coverage ≥ 5; Consensus loci: number of loci with depth ≥ 5 and passed paralog filter; Loci in final dataset: number of loci available for 18 taxa or more.

Gene	Minimum lenght	Maximum lenght	Aligned length	Polymorphic sites
COI	621	621	621	165
16S	324	340	357	59
5.8S-ITS2	836	869	906	56
28S	564	565	566	7
Total	2348	2383	2451	287

Table 2: Sequence lengths and numbers of variable sites of COI, 16S, 5.8S-ITS2, 28S and the combined datasets.

Model	Description	Species number	ML	BF	Rank
0. Base scenario	Species delimited in Razkin et al. (under review) (Figure 2-a)	9	-4505,8	-	1
1. Clustering 1	*P. rupestris* +*P. saxatilis* (Figure 2-b)	8	-4656,7	301,8	4
2. Clustering 2	*P. jaenensis* + *P. chorismenostoma* + *P. cephalonica* (Figure 2-c)	7	-4806,7	601,8	5
3. Split 1	*P. pusilla* = *P. pusilla*_west + *P. pusilla*_east (Figure 2-d)	10	-4524,1	36,6	3
4. Split 2	*P. jaenensis* = *P. jaenensis*_west + *P. jaenensis*_east (Figure 2-e)	10	-4515,5	19,4	2

Table 3: Results for BFD* species delimitation: ML (marginal likelihood); BF (Bayes factor).

TEST	P1	P2	P3	O	Range Z	Nsig/n (α= 0.05, 0.01)	Allele pattern (sigD)	Species involved in introgression	Range nloci	Range pdisc
1 - 4taxon	*P. rupestris*	*P. saxatilis*	*P. pusilla*	*P.* sp1	(0.47, 2.63)	**8/24, 1/24**	ABBA	*P. pusilla* - *P. saxatilis*	(2272, 3040)	(0.1, 0.12)
2 - 4taxon	*P. chorismenostoma*	*P. jaenensis*	*P. cephalonica*	*P. pusilla*	(0.05, 1.51)	0/24, 0/24			(1716, 2704)	(0.12, 0.14)
3 - 4taxon	*P. chorismenostoma*	*P. jaenensis*	*P.* cf. *hierosolymitana*	*P. pusilla*	(0.03, 1.67)	0/8, 0/8			(1755, 2510)	(0.06, 0.07)
4 - 4taxon	*P. chorismenostoma*	*P. jaenensis*	*P.* sp1	*P. pusilla*	(0.84, 2.2)	**2/4**, 0/4	BABA	*P. chorismenostoma* - *P.* sp1	(1302, 1675)	(0.07, 0.09)
5 - 4taxon	*P. chorismenostoma*	*P. jaenensis*	*P.* sp2	*P. pusilla*	(0.98, 2.64)	**2/8, 1/8**	BABA	*P. chorismenostoma* - *P.* sp2	(1889, 2540)	(0.11, 0.12)
6 - 4taxon	*P. cephalonica*	*P. chorismenostoma*	*P.* cf. *hierosolymitana*	*P. pusilla*	(0.2, 2.8)	**6/12, 1/12**	BABA	*P. cephalonica* - *P.* cf. *hierosolymitana*	(1913, 2494)	(0.07, 0.09)
7 - 4taxon	*P. cephalonica*	*P. chorismenostoma*	*P.* sp1	*P. pusilla*	(0.17, 0.58)	0/6, 0/6			(1420, 1664)	0.09
8 - 4taxon	*P. cephalonica*	*P. chorismenostoma*	*P.* sp2	*P. pusilla*	(1.6, 2.8)	**9/12, 1/12**	BABA	*P. cephalonica* - *P.* sp2	(2072, 2515)	(0.15, 0.16)

Table 4: Results of the four taxon D-statistic tests showing the range of Z-scores ("Range Z"); number of significant replicates ("Nsig/n"); main allele pattern in significant replicates ("Allele pattern (sigD)"); species involved in introgression; range of number of available RAD loci ("Range nloci"); and range of percentage of non concordant sites over all possible replicates ("Range pdisc").

							D_12			D_1			D_2			
TEST	**P1**	**P2**	**P3_1**	**P3_2**	**O**	**Range Z**	**Nsig/n (α= 0.05, 0.01)**	**Allele pattern (sigD)**	**Range Z**	**Nsig/n (α= 0.05, 0.01)**	**Allele pattern (sigD)**	**Range Z**	**Nsig/n (α= 0.05, 0.01)**	**Allele pattern (sigD)**	**Range nloci**	**Range pdisc**
1 - part	*P. rupestris*	*P. saxatilis*	*P. pusilla*$_1$	*P. pusilla*$_2$	*P.* sp1	(0.63, 2.87)	**13/36, 4/36**	ABBBA (13)	(0.05, 4.06)	**4/36, 2/36**	BABAA (2), ABBAA (2)	(0.1, 4.47)	**4/36, 2/36**	BAABA (4)	(1860, 2551)	(0.11, 0.13)
5 - part	*P. chorismenostoma*	*P. jaenensis*	*P.* sp2$_1$	*P.* sp2$_2$	*P. pusilla*	(1.58, 2.22)	**1/4,** 0/4	BABBA (1)	(1.23, 2.89)	**3/4, 1/4**	BABAA (3)	(0.16, 2.4)	0/4, 0/4		(1757, 2284)	(0.12, 0.13)
6 - part	*P. cephalonica*	*P. chorismenostoma*	*P.* cf. *hierosolymitana*$_1$	*P.* cf. *hierosolymitana*$_2$	*P. pusilla*	(0.37, 2.47)	**1/6,** 0/6	BABBA (1)	(0.1, 0.38)	0/6, 0/6		(0.7, 2.86)	**1/6, 1/6**	BAABA (1)	(1834, 2138)	(0.08, 0.09)
8 - part	*P. cephalonica*	*P. chorismenostoma*	*P.* sp2$_1$	*P.* sp2$_2$	*P. pusilla*	(1.58, 2.38)	**1/6,** 0/6	BABBA (1)	(0.04, 0.78)	0/6, 0/6		(0.24, 1.29)	0/6, 0/6		(1926, 2250)	(0.17, 0.18)

Table 5: Results of the partitioned D-statistic tests showingthe range of Z-scores ("Range Z"); number of significant replicates ("Nsig/n"); main allele pattern in significant replicates ("Allele pattern (sigD)"); range of number of available RAD loci ("Range nloci"); and range of percentage of non concordant sites over all possible replicates ("Range pdisc").

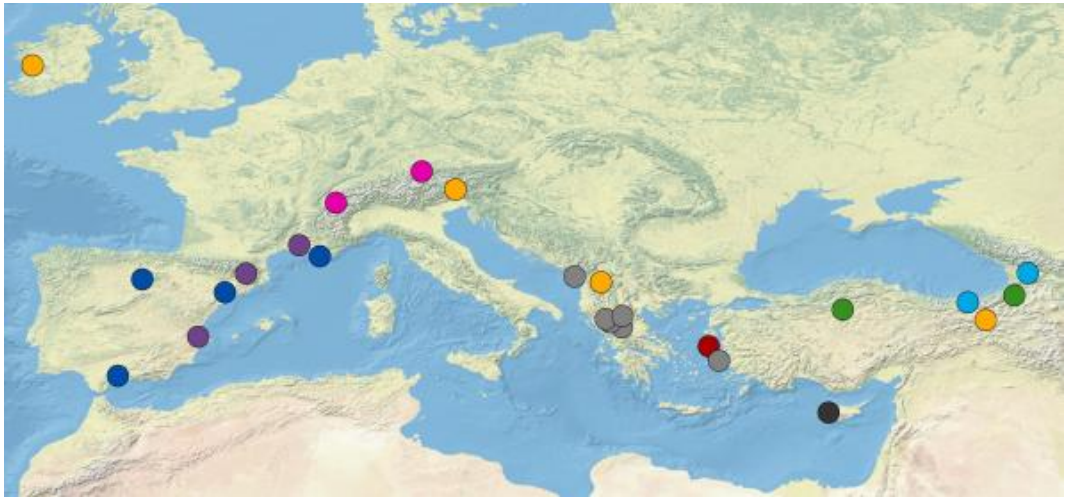

RADseq

species delimitation

interspecific hybridization

phylogeny

Pyramidula

Highlights:

- RADseq successfully resolved taxonomic and phylogenetic problems in *Pyramidula*
- Phylogenetic relationships among species were fully resolved
- D-statistics provided no or weak evidence of ancestral interspecific hybridization
- The best species delimitation scenario distinguished nine species in Europe